Ocean Dynamics (2017) 67:751–766
DOI 10.1007/s10236-017-1057-0

On the predictability of high water level along the US East Coast: can the Florida Current measurement be an indicator for flooding caused by remote forcing?

Tal Ezer[1] · **Larry P. Atkinson**[1]

Received: 2 August 2016 / Accepted: 5 April 2017 / Published online: 24 April 2017

Abstract Recent studies show that in addition to wind and air pressure effects, a significant portion of the variability of coastal sea level (CSL) along the US East Coast can be attributed to non-local factors such as variations in the Gulf Stream and the North Atlantic circulation; these variations can cause unpredictable coastal flooding. The Florida Current transport (FCT) measurement across the Florida Straits monitors those variations, and thus, the study evaluated the potential of using the FCT as an indicator for anomalously high water level along the coast. Hourly water level data from 12 tide gauge stations over 12 years are used to construct records of maximum daily water levels (MDWL) that are compared with the daily FCT data. An empirical mode decomposition (EMD) approach is used to divide the data into high-frequency modes (periods $T < \sim 30$ days), middle-frequency modes (~ 30 days $< T < \sim 90$ days), and low-frequency modes (~ 90 days $< T < \sim 1$ year). Two predictive measures are tested: FCT and FCT change (FCC). FCT is anti-correlated with MDWL in high-frequency modes but positively correlated with MDWL in low-frequency modes. FCC on the other hand is always anti-correlated with MDWL for all frequency bands, and the high water signal lags behind FCC for almost all stations, thus providing a potential predictive skill (i.e., whenever a weakening trend is detected in the FCT, anomalously high water is expected along the coast over the next few days). The MDWL-FCT correlation in the high-frequency modes is maximum in the lower Mid-Atlantic Bight, suggesting influence from the meandering Gulf Stream after it separates from the coast. However, the correlation in low-frequency modes is maximum in the South Atlantic Bight, suggesting impact from variations in the wind pattern over subtropical regions. The middle-frequency and low-frequency modes of the FCT seem to provide the best predictor for medium to large flooding events; it is estimated that ~10–25% of the sea level variability in those modes can be attributed to variations in the FCT. An example from Hurricane Joaquin (September–October, 2015) demonstrates how an offshore storm that never made landfall can cause a weakening of the FCT and unexpected high water level and flooding along the US East Coast. A regression-prediction model based on the MDWL-FCT correlation shows some skill in estimating high water levels during past storms; the water level prediction is more accurate for slow-moving and offshore storms than it is for fast-moving storms. The study can help to improve water level prediction since current storm surge models rely on local wind but may ignore remote forcing.

Keywords Gulf Stream · Florida Current · Sea level · Climate change · Coastal flooding

This article is part of the Topical Collection on the *8th International Workshop on Modeling the Ocean (IWMO), Bologna, Italy, 7–10 June 2016*

Responsible Editor: Leo Oey

✉ Tal Ezer
tezer@odu.edu

[1] Center for Coastal Physical Oceanography, Old Dominion University, 4111 Monarch Way, Norfolk, VA 23508, USA

1 Introduction

The geostrophic balance implies that sea level slope across strong ocean currents is proportional to the surface flow speed, so in the case of western boundary currents like the Kuroshio in the Pacific Ocean or the Gulf Stream (GS) in the Atlantic Ocean, variations in the flow speed or position of the offshore current can impact variations in coastal sea level (CSL) or vice versa (when variations in sea level influence the current speed). In general, a weakening in a western boundary current transport will increase coastal sea level in the onshore side of the current (and decrease sea level offshore). This mechanism was recognized a long time ago. Early observations (Montgomery 1938; Blaha 1984) and models (Ezer 1999, 2001; Sturges and Hong 2001) suggest that CSL along the US East Coast is influenced by offshore (remote) variations in the intensity of the GS or the Atlantic Ocean. For example, a potential climate change-related slowdown of the GS (Sallenger et al. 2012; Ezer et al. 2013) which is part of the Atlantic Meridional Overturning Circulation (AMOC; McCarthy et al. 2012; Smeed et al. 2013; Srokosz and Bryden 2015) may cause accelerated sea level rise and increased risk of flooding along the US East Coast (Levermann et al. 2005; Boon 2012; Ezer and Corlett 2012; Sallenger et al. 2012; Yin and Goddard 2013; Goddard et al. 2015; Ezer and Atkinson 2014). A significant correlation between the GS and CSL is found on a wide range of timescales, from daily variations (Ezer 2016, 2017) to decadal and multidecadal variations (Ezer 2015). A simple dynamic balance analysis of along coast geostrophic current (Ezer et al. 2013) showed that the GS may influence CSL either directly when sea level slope across the GS affect CSL on the onshore side or by the generation of onshore/offshore barotropic transport variations when the GS changes its strength or position. These barotropic signals can generate coastal-trapped waves that affect long stretches of coasts within short period of time (Huthnance 2004; Hughes and Meredith 2006), as demonstrated by idealized numerical simulations of the GS (Ezer 2016, 2017). In view of these past studies, two indicators are evaluated: the GS strength itself and changes in the GS flow.

The relation between CSL and offshore variations is not fully understood since it involves various factors such as variations in AMOC and the GS transport, westward propagating planetary waves (Ezer 1999; Sturges and Hong 2001; Domingues et al. 2016), and variations in the thermo-haline structure and wind pattern in the Atlantic Ocean (Srokosz and Bryden 2015). In addition, variations in atmospheric pressure and associated inverted barometer (IB) effects can significantly influence CSL variability on interannual and multidecadal timescales (by as much as 10–30% of the sea level signal according to Piecuch and Ponte 2015). An interesting result of several studies (e.g., Ezer 2013; Piecuch et al. 2016; Woodworth et al. 2016) is the different response of CSL to forcing between the coasts north of Cape Hatteras (MAB and GOM in Fig. 1) and the coasts south of Cape Hatteras (SAB). There are differences in the coastline and wind pattern between the two regions, but the ocean dynamics may also play a role since the GS path has much larger variability after separating from the coast at Cape Hatteras, while in the SAB, the GS is flowing close to the coast and thus may be a more dominant force than other offshore influences. Piecuch et al. (2016), for example, show that north of Cape Hatteras, barotropic dynamics, and wind stress over the continental shelf may be responsible for large part of the CSL variability on interannual and decadal timescales. The CSL is also closely related to the North Atlantic Oscillations (NAO) and Atlantic circulation patterns (Ezer et al. 2015; Woodworth et al. 2016). The coasts north of Cape Hatteras also see larger recent accelerations in sea level rise rates, a result often attributed to ocean dynamics influence (Boon 2012; Sallenger et al. 2012; Ezer and Corlett 2012; Yin and Goddard 2013). The above discussion and studies focused mostly on long-term variability on timescales of interannual to multidecadal, but less attention is given to short-term variability on timescales of days to a year or so, which provides motivation of this study.

On short-term timescales, extreme events such as tropical storms and hurricanes are associated with low air pressure and thus have strong IB impact as well. Because storms involve a combination of large changes in both wind and pressure, they impact CSL through storm surge and IB effects that are not easy to separate. One mechanism in which large-scale offshore signals (e.g., due to changes in wind, pressure, or ocean currents) are transmitted to the shelf is through the generation of coastal-trapped waves (Huthnance 2004). This mechanism can result in coherent CSL anomalies that are observed along many different coasts (Hughes and Meredith 2006), and recently, this mechanism was demonstrated by a numerical ocean model of the US East Coast (Ezer 2016, 2017). Zhao and Johns (2014) shows that wind-driven variations over the subtropical gyre can also result in coherent sea level variations along the GS path over thousands of kilometers. The complex and unpredictable nature of remote forcing of coastal sea level makes it very difficult to accurately simulate coastal sea level and flood risk, since coastal and storm surge models rely on local wind forcing, but may neglect remote factors, as those mentioned above. As a result, unpredictable coastal flooding often occurs, and these events increase in recent years due to sea level rise (Mitchell et al. 2013; Ezer and Atkinson 2014; Sweet and Park 2014).

One of the longest, and almost continuous, measurements of Atlantic Ocean variability (since the early 1980s) is the cable measurements of the Florida Current transport (FCT) across the Florida Straits (Baringer and Larsen 2001; Meinen et al. 2010; Domingues et al. 2016). This measurement can capture some of the variations in wind and ocean circulation over the Atlantic Ocean, so it may provide an indication for the remote forcing of CSL that cannot be directly observed. The current study follows on the footsteps of previous studies that found significant correlations between FCT and CSL in observations (Ezer et al. 2013; Park and Sweet 2015) and in models (Ezer 2001, 2016). This relation provides motivation to test the proposition that CSL prediction can be improved if remote offshore forcing is considered through easily obtained existing measurements, such as the FCT

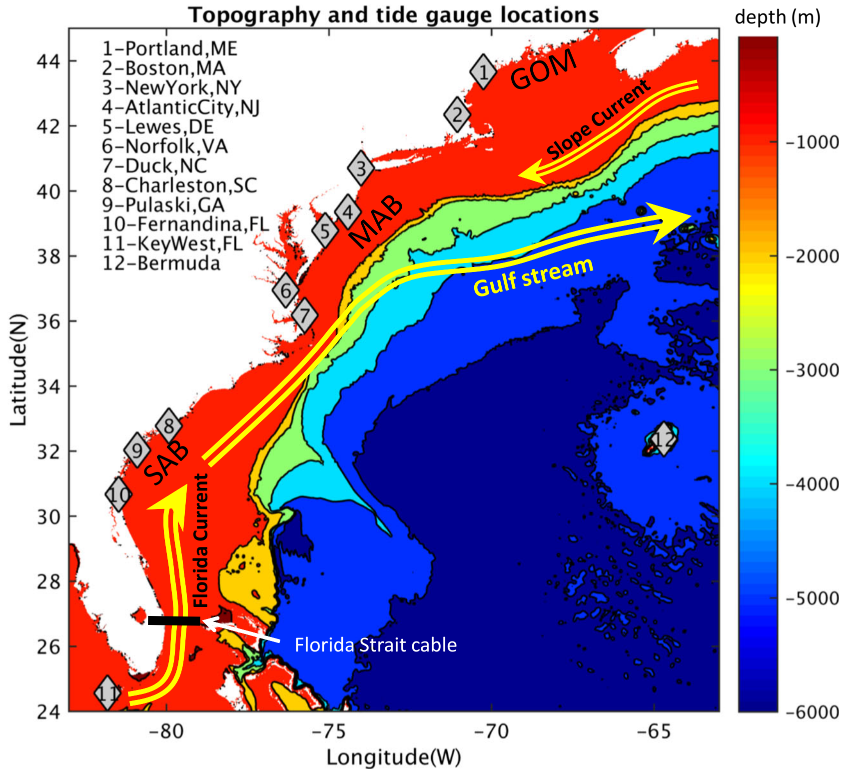

Fig. 1 Topographic map (based on ETOPO1 data) of the study area (water depth in color) and locations of 12 tide gauge stations. Three regions discussed in the text, the Gulf of Maine (*GOM*), the Mid-Atlantic Bight (*MAB*), and the South Atlantic Bight (*SAB*), are indicated. Schematic of the major currents in the region are depicted in *yellow arrows*. The location of the Florida Current cable measurement in the Florida Strait is indicated by a *black heavy line*

record. The study is focused on two main goals: (1) to quantify the FCT-CSL relation in terms of its spatial variations along the coast and the timescales involved and (2) to test the predictability of high water level and increased flood risk using the FCT measurement as an indicator. The paper is organized as follows: First, the data and the analysis methods are described in Sect. 2; then, the results for different coastal locations are presented in Sect. 3, and in particular, an example of the impact of one offshore storm is demonstrated in Sect. 4, following by discussion and conclusions in Sect. 5.

2 Data and analysis methods

Hourly sea level records from 12 tide gauge stations were obtained from NOAA (http://opendap.co-ops.nos.noaa.gov/dods/), and the locations are shown in Fig. 1. The data represent five different regions, two stations in the Gulf of Maine (GOM), five stations in the Mid-Atlantic Bight (MAB), three stations in the South Atlantic Bight (SAB), one station (Key West) between the Florida Strait and the Gulf of Mexico, and one station (Bermuda) on the eastern side of the GS (Fig. 1). Bermuda station is the only location not on the US coast; it was chosen because past studies show that sea level in Bermuda can capture signals of westward propagating planetary waves (Sturges and Hong 2001; Ezer 1999, 2001) and that the sea level difference between Bermuda and the US coast can capture variations in the GS and AMOC (Ezer 2015). Twelve years of data (2004–2015) provides ~105,000 hourly measurements for each station. From the hourly data, a maximum daily water level (MDWL) record is obtained, providing a record of ~4400 data points for each station. The focus is on high water level that can potentially cause flooding. For typical, quiet periods of time, when water level is dominated by the daily tides, the value of MDWL should be close to the MHHW, but for a period when a storm is passing, for example, MDWL may be considerably higher than MHHW. Note that all water level values hereafter are relative to MHHW, unless otherwise indicated.

While the tide gauge sea level records are much longer than the records analyzed here (the average length of the stations is ~85 years), longer records would require to consider the impact of sea level rise (local rates for those stations are in the range ~2.5–4.5 mm year^{-1}) on acceleration in flooding, as has been documented before (Mitchell et al. 2013; Ezer and Atkinson 2014; Sweet and Park 2014). As an example, Fig. 2a shows the annual hours of moderate flooding in Norfolk, when water level reaches at least 0.6 m above MHHW (some major storms that caused flooding in each year are also listed, but additional flooding also occurred due to smaller storms and high tides). During the almost 90 years of data at this station, half of the most flooded years occurred in the last decade. The large increase in flood hours in Norfolk is mostly due to the combination of global sea level rise and significant land subsidence in the coasts of the lower Chesapeake Bay. Land subsidence in this area is due to

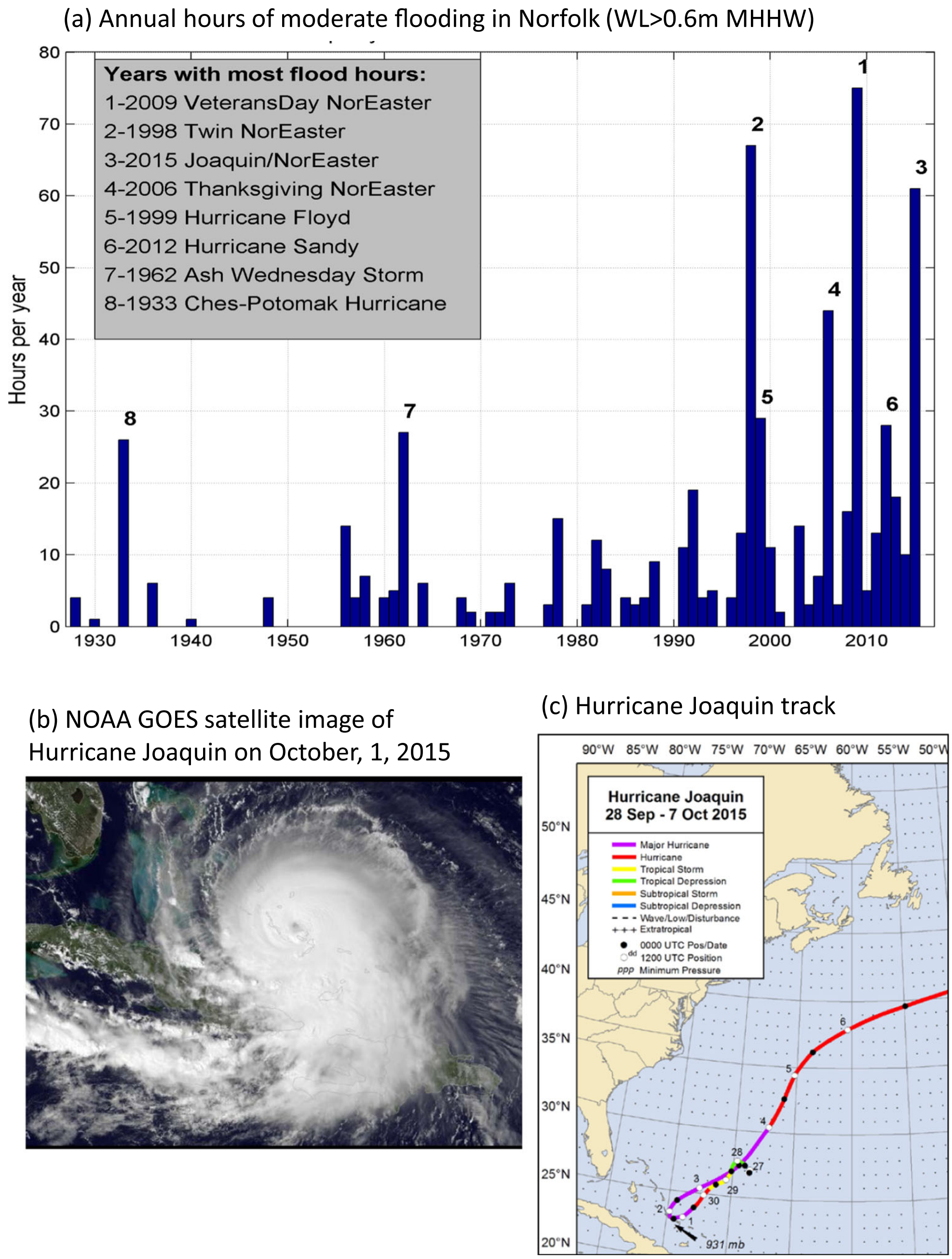

Fig. 2 **a** The number of hours per year that water level in Sewells Point (Norfolk, VA) is at least 0.6 m above mean higher high water (MHHW); this level corresponds to a moderate street flooding. The rank of the top 8 years with the most flooding is listed, as well as some major storms in each year. **b**, **c** Satellite image of Hurricane Joaquin taken on October 1, 2015 and the hurricane's track between September 28 and October 7, 2015, respectively (from the NOAA report by Berg 2016)

combinations of glacial isostatic adjustment (GIA) and groundwater extraction; estimations of land subsidence rates from observations and models are in the range of 1–2.5 mm year^{-1} (Eggleston and Pope 2013; Miller et al. 2013; Karegar et al. 2016). Therefore, because of the large local sea level rise, relatively weak storms or even higher than normal tides can now cause much more flooding than past years when sea level was lower. The third most flooded year on record was 2015, and most of the floods this year happened during about 2 weeks in late September to early October, when Hurricane Joaquin developed in the subtropics (Fig. 2b). Even though this hurricane later moved northeastward and never came close to the coast (Fig. 2c), its remote influence on the coast was substantial with significant coastal flooding in many places along the SAB and MAB coasts (considerable rain from a nor'easter storm was also in play at the time). This particular storm was chosen to demonstrate a case where offshore storm influenced the GS and apparently CSL; this case will be discussed in detail later.

The daily Florida Current transport from cable measurements across the Florida Strait at 27° N (Baringer and Larsen 2001; Meinen et al. 2010) is obtained from the NOAA/Atlantic Oceanographic and Meteorological Laboratory web site (www.aoml.noaa.gov/phod/

floridacurrent/); see the location in Fig. 1. The data include the periods 1982–1998 and 2000–2016 with a large gap of about 2 years and several shorter gaps of 1–2 weeks; here, only the data for 2004–2015 is used. Numerous studies (see list of references in the NOAA/AOML site) analyzed the FCT record, its seasonal and decadal variability, as well as its connections with basin-scale variability of AMOC (McCarthy et al. 2012) and with the NAO index (the NAO index is often anti-correlated with variations of the FCT; Baringer and Larsen 2001).

The MDWL and FCT records have variations on different timescales, from daily and seasonal to decadal variability. Since storms are particularly irregular in their frequency, standard analysis methods (Thomson and Emery 2014) that assume an oscillatory behavior with a particular frequency (e.g., harmonic or spectral analysis) will provide only limited information on extreme events. Nevertheless, Fig. 3 is an example of the spectral analysis and coherence between MDWL in Norfolk and the FCT record (the power spectral density calculation is based on Welch's averaged estimate with Hamming windows). The sea level data shows significant peaks from the annual and semiannual timescales to cycles of about 2 weeks and ~1 month (Fig. 3a), while the FC record has maximum energy at the annual cycle with other peaks that are less significant (Fig. 3b). Significant coherences between the two time series are found at various frequencies from periods of ~10 days to ~1 year with maximum correlation at timescales of ~2–3 months (Fig. 3c). The typical phase difference between the two is ~100°–180° (Fig. 3d), implying that higher sea level is expected when FC transport is low, in agreement with the many studies mentioned before.

The spectral analysis (Fig. 2) is quite a common and useful tool, but it does not provide information on non-stationary processes, such as extreme CSL events that do not happened at regular intervals. Another analysis method that is based on the non-stationary EMD (Huang et al. 1998) can be used to separate the data into different timescales and capture variations that change with time. The EMD method has been used for numerous sea level analyses around the world (Ezer and Corlett 2012; Ezer 2013, 2015; Chen et al. 2014; Park and Sweet 2015), and more details on the method can be found in those studies. Using a repeated sifting process, the EMD composes a time series into N oscillating modes and a residual trend (the trend can be linear or any function that has no more than one extremum). The number of modes depends on the length of the record and its variability, and in our case of 12 years of daily data, mode 0 denotes the original time series, modes 1–11 represent the oscillatory modes from high to low frequency, and mode $N = 12$ is the residual. Keep in mind that in each mode, the amplitude and frequency are not constant, but time-dependent. It is constructive to group modes together into different frequency bands, so here, the data are divided into four groups: high frequency (modes 1 and 2; periods less than 3 months), middle frequency (modes 3 and 4; periods of ~3–9 months), low frequency (modes 5–7; periods of ~9–12 months), and lowest frequency (modes 8–12; periods over 1 year, including the trend). An EMD analysis has been applied to all the 12 MDWL records and to the FCT record, and cross-correlations between the water level and FCT are calculated for each station and for each frequency band. The cross-correlations indicate if there is a significant correlation between MDWL and FCT and if so at what lag difference. Attention is given to large peaks in correlation that are closest to the zero lag. Negative lags imply that variations in FCT are ahead of variations in water level (thus providing the potential for predicting coastal sea level from the FCT record). Positive lag when signals are detected first in sea level at northern coasts and only later at the FCT can indicate large-scale forcing that excites southward propagating coastal-trapped waves (Ezer 2016). It is emphasized though that correlation does not mean causation, but nevertheless, significant correlation may provide some predictive tool. Note that because of the large number of points in the daily records, correlation above R ~0.03 is statistically significant at the 95% confidence level if time series are independent, but if the reduction of the number of degrees of freedom in EMD is taking into account, correlations at the low-frequency modes are estimated to require a value of R ~0.1 to be statistically significant. However, even if the correlation is statistically different than zero at 95% of the time, $R = 0.1$ means that only ~1% of the variability is captured. In the case of the sea level-FC relation, at some frequencies, correlations are as large as R ~0.5, which implies that ~25% of the sea level variability may be represented by the FC variability. For high-frequency and medium-frequency modes, the impact of the EMD on the significance of the correlation is negligible since the effective degrees of freedom depend on the autocorrelation scale (Thiebaux and Zwiers 1984).

3 The relation between the Florida Current transport and high water level along the coast

Examples of the EMD calculations for Boston, Norfolk, and Charleston, representing the GOM, MAB, and SAB, respectively, are shown in Figs. 4, 5, and 6. In Boston (Fig. 4), statistically significant correlations with FCT are seen in the high-frequency band (modes 1 and 2) and the low-frequency band (modes 5–7); at both bands, positive lags for high correlation of first peak indicate a potential signal that is seen in water level ahead of the FCT; thus, the sea level signal there is likely coming from oceanic or atmospheric signals not directly caused by the FCT. The highest correlation (~−0.7) is found at the lowest frequency band (modes 8–12) and is related to the downward trend in the FCT, while sea level is rising; this trend has been discussed before (Ezer 2013; Ezer et al. 2013), so the

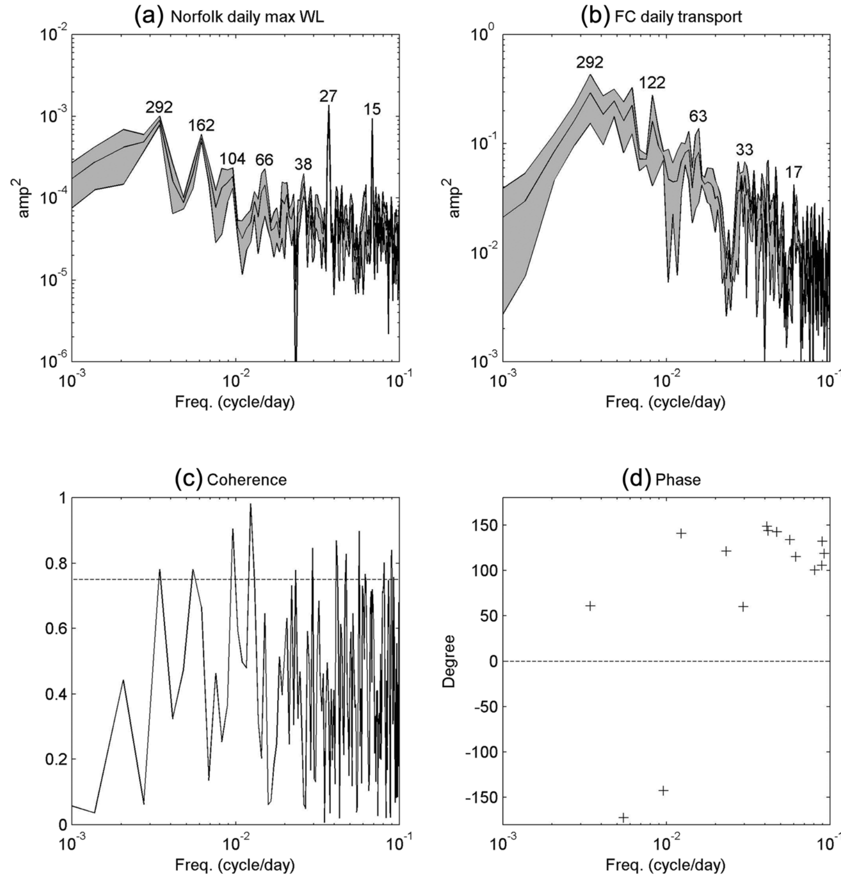

Fig. 3 Spectral analysis of **a** daily maximum water level in Norfolk (in m^2) and **b** daily Florida Current transport (in Sv^2); *gray area* represents the 95% confidence interval, and the *numbers* indicate the period (in days) of particular peaks. The coherence and phase difference between the two time series are shown in **c** and **d**; the estimated 95% confidence level in the coherence is indicated by the *horizontal dash line* in **c**, and phase is only shown for peaks with significant coherence

focus here will only be on the three other frequency bands. At Norfolk (Fig. 5), significant negative cross-correlation with small positive lag is seen in all three bands, though at the low-frequency band, another larger peak with correlation close to 0.5 at negative lag is also seen. The negative correlation means that water level at Norfolk is higher when the FCT is weaker, a phenomenon indicated by previous studies (Ezer et al. 2013; Ezer and Atkinson 2014) and confirms by the spectral coherence analysis (Fig. 2); this station will be further explored later. At Charleston (Fig. 6), large negative correlation with almost no lag is seen in all three frequency bands—this result may be explained by the fact that this station is located downstream from the Florida Straits where the Florida Current flows along the SAB coast, so any weakening in the FCT would cause a rise/fall in sea level on/off shore. This result has been suggested before based on early observations (Blaha 1984), but here, it is shown that the impact of the FCT on coastal sea level in the SAB applies to a wide range of timescales from few days to seasonal. Interannual to decadal variations in the coastal sea level in the MAB region are better correlated with the *change* in the Gulf Stream transport than with the Gulf Stream strength itself (Ezer et al. 2013). Therefore, the FCT change (FCC in Sv change per day) is also evaluated as a potential predictive for high water level. Figure 7 shows an example of the EMD in Norfolk, comparing FCC and MDWL. The high negative correlation with zero lag for the high-frequency modes indeed indicates that short-term flooding in Norfolk may be predicted from a weakening FCT observed at the same time, which was anecdotally shown before (Ezer and Atkinson 2014). Middle-frequency and low-frequency modes also show statistically significant negative correlations with FCC, but with negative lag, meaning that high water in Norfolk may be predicted a few days in advance from FCC.

Figure 8 summarizes the correlations and the lags between the FCT and all the 12 stations, and Fig. 9 summarizes the correlations between FCC and the 7 stations in the MAB and SAB (the rest of the stations do not show significant correlation with FCC). In the high-frequency modes, FCT-MDWL correlations are all negative with a maximum (absolute value) at Norfolk and decreasing correlations farther north or south (Fig. 8a), while for low-frequency modes, the correlations are always positive with larger values in the south near the FCT measurement (Fig. 8c). The lag between FCT and MDWL also shows significant differences between the high-frequency (Fig. 8b) and low-frequency (Fig. 8d) bands and a clear regional pattern. High-frequency variability in sea level in the SAB has zero lag with FCT (indicating coherent FCT variations along the coast of the SAB) and only short lag of 2–3 days in the MAB, while farther north correlations are smaller

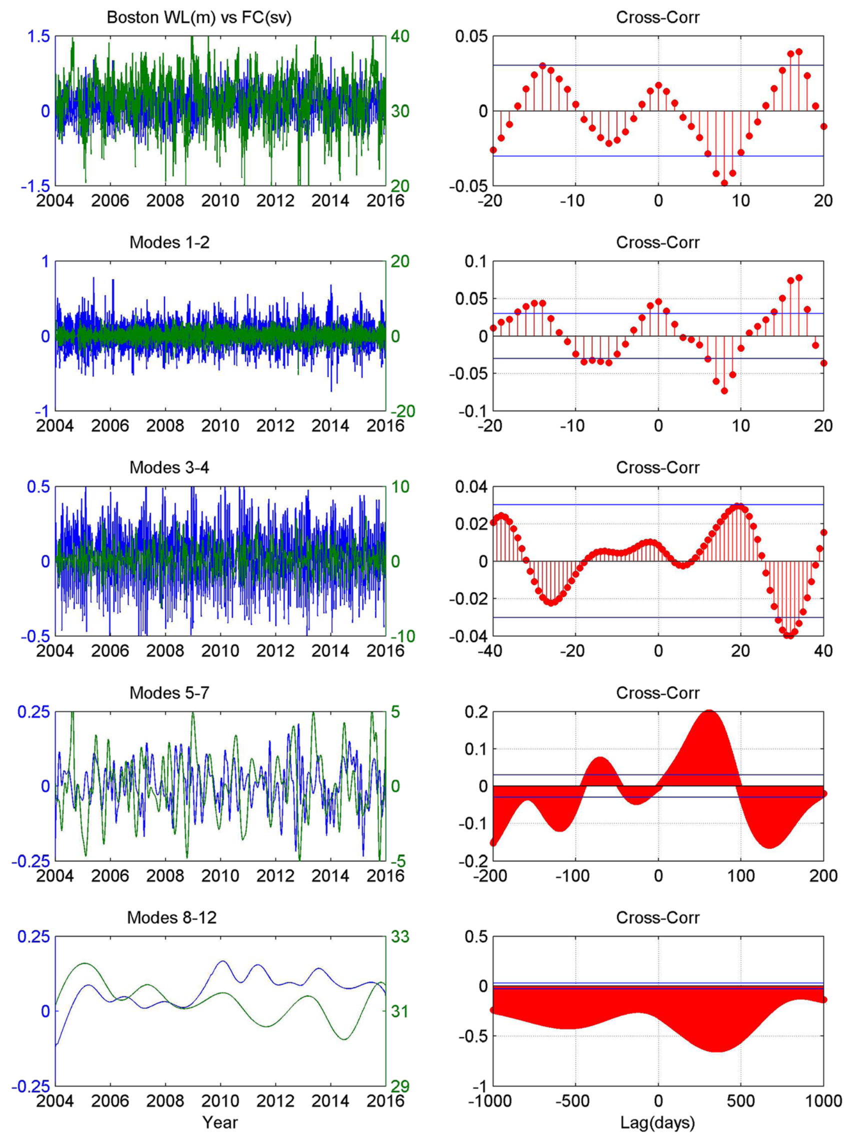

Fig. 4 Maximum daily water level in Boston (*blue lines*; in m) versus the Florida Current transport (*green lines*; in Sv, 1 Sv = 10^6 m^3 s^{-1}). The *top-left panel* is the original record, and the *second to fourth lower panels* are for the EMD modes of "high frequency," "middle frequency," "low frequency," and "lowest frequency" (see text for definitions). The *panels on the right* are the corresponding cross-correlation coefficients (*red dots* and *vertical lines*) as a function of lag difference (e.g., in the *fourth panel* on the right positive correlation of 0.2 with positive lag of 62 days means that high water level appears 62 days ahead of increased in FCT). The *horizontal lines in the right panels* indicate the standard 95% confidence intervals (see text for the potential reduction of the number of degrees of freedom in the EMD, considered later)

and lags are larger (Fig. 8b). Low-frequency variability in sea level has similar high correlations (0.35–0.45; Fig. 8c) and similar lags (60–80 days; Fig. 8d) for stations from Key West, FL to Atlantic City, NJ, pointing to potential large-scale forcing from the Atlantic Ocean that creates a coherent pattern along some 2000-km stretch of the coast. An opposite lag in Bermuda also points to large-scale patterns since the sea level difference between Bermuda and the US coast is closely related to the strength of the Gulf Stream and AMOC (Ezer 2015). North of New York, the pattern of both high-frequency and low-frequency variability is clearly different than those of the MAB and SAB, so the dynamic mechanism may be different, potentially seeing impact of signals coming from the Labrador Sea and the Slope Current (Fig. 1). However, variations in the Slope Current are not independent from variations in the GS (Rossby et al. 2010; Ezer 2013, 2015), so it is difficult to distinguish between the forcing of the two currents which are connected to each other through the recirculation gyre north of the GS.

In Fig. 9, the focus is on the impact of FCC on the MAB and SAB, showing the three frequency bands. It is interesting to note that unlike correlations with FCT (Fig. 8), correlations with FCC have much more coherent spatial pattern—the correlations are all negative and lags are mostly negative (i.e., FCC signal is ahead of the coastal sea level signal). The maximum correlation for the high-frequency band is in the lower MAB (Norfolk, VA, and Duck, NC) near the separation point of the GS, and there is zero lag there (Fig. 9b), suggesting that the GS may amplify signals near Cape Hatteras. The impact of the sharp change of the coastline at Cape Hatteras on signals propagating along the coast has been shown in other studies as well (Ezer 2013, 2016). The change in the sign of the lag from positive in the north to negative in the south suggests a southward propagation of signals, which is consistent with coastal-

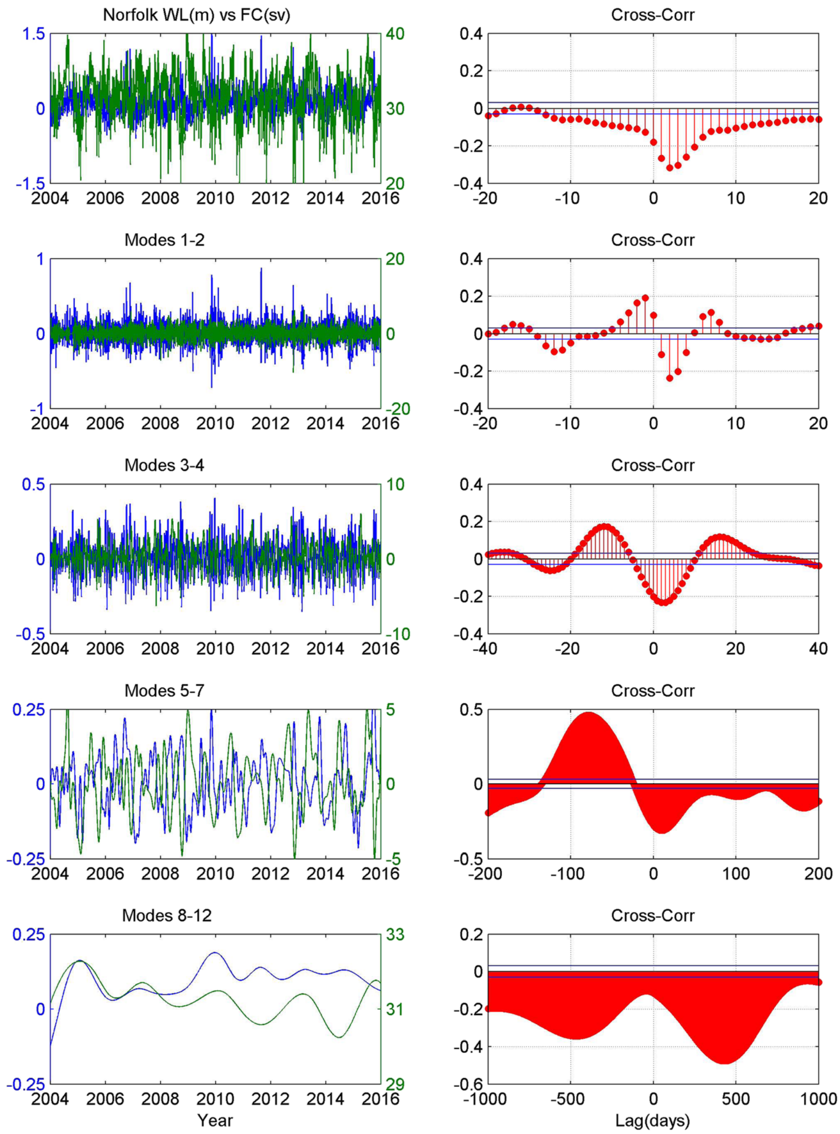

Fig. 5 Same as Fig. 3, but for water level in Norfolk

trapped waves in the northern hemisphere (Huthnance 2004; Ezer 2016). The medium-frequency and low-frequency bands show larger correlations in the south, suggesting potential sources in the subtropical region such as Rossby waves and changes in wind pattern over the subtropical gyre (Ezer 1999, 2001; Sturges and Hong 2001).

One of the goals of the study is to test the ability of the FCT observations in providing warning for anomalously high water that can cause unpredictable flooding in places such as Norfolk (Ezer and Atkinson 2014). Therefore, instead of looking at the entire MDWL record, as done so far, only days with particular high water level are analyzed for Norfolk in Fig. 10. Three water levels are extracted: (1) water level of 0.2 m over MHHW, representing tides that are slightly higher than normal and only very minor flooding is seen in some streets—during the 12-year record, this happened ~26% of the time; (2) water level of 0.5 m over MHHW, which is close to the "nuisance" flooding level in Norfolk as defined by NOAA (Park and Sweet 2015); about 2.5% of the days experienced such water level, which can cause minor to moderate flooding to many streets in Norfolk; and (3) water level of 0.8 m over MHHW, which occurred only ~0.5% of the time (22 days during the 12-year study period), but can cause major flooding of large sections of the city. The results show that the high-frequency modes of the FCT data are not good predictors for high water level (blue bars in Fig. 10), while medium-frequency (green) and low-frequency (red) modes are better indicators with statistically significant correlations. For simplicity, all predictions are based on zero lag, though higher correlations can be found if lag is adjusted for each frequency band. For the major flood cases, the correlation coefficient indicates that ~40% of the high water variability can be attributed to the low-frequency modes of the FCT. The EMD thus provides a way to filter out high-frequency variability that

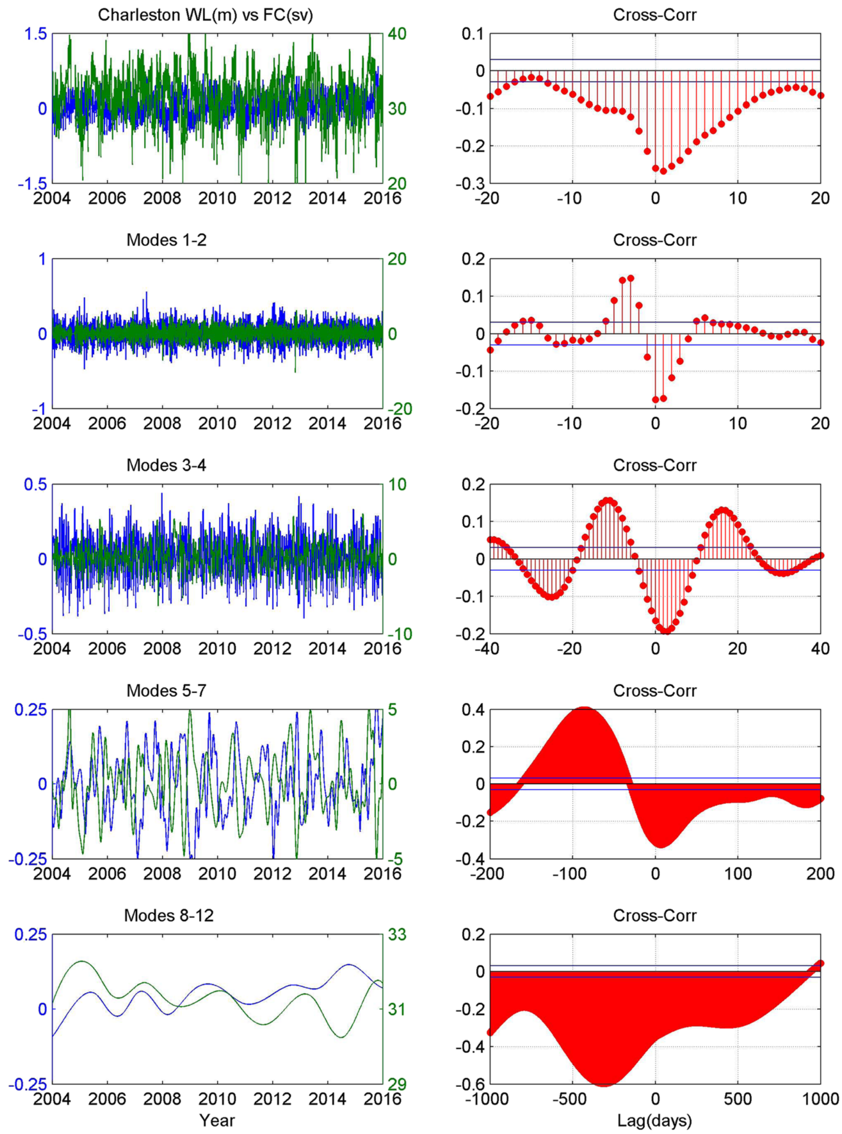

Fig. 6 Same as Fig. 3, but for water level in Charleston

does not contribute to major flooding. Since the correlations increase quite linearly with high water level, interpolation to other water levels is straight forward, though for a much higher water level of storm surge, there is not enough data for significant statistics (e.g., when Hurricane Irene passed over Norfolk in 2011, water level reached ~1.5 m over MHHW, about twice the highest water level considered here).

Can the correlations shown in Fig. 10 be used for prediction of high water level? As an example, the linear regression coefficients (a and b) for water level of 0.8 m above MHHW in Norfolk for the low-frequency EMD modes of FCT have been obtained. Then, the predicted water level is estimated by WLp = $A[a(\mathrm{FCT}) + b]$, where A is a constant scale factor based on the ratio between the mean high water of the original data and the low-frequency modes (to account for the reduction of amplitude in low-frequency modes). Figure 11 compares the predicted and observed high water level. During 2004–2015, there were 21 days with water levels greater than 0.8 m over MHHW, and the regression calculation predicts that 16 of them reach this level (red circles in Fig. 11), while in five cases, the prediction underestimated the water level (green triangles in Fig. 11); however, even in the underpredicted cases, the regression model shows higher than normal water level of at least 0.2 m. It is interesting to note that such calculations can predict quite well high water level associated with either slow-moving nor'easters or offshore storms that did not make landfall. For example, in November 21, 2006, during the "Thanksgiving Day nor'easter" ("T" in Fig. 11), observed water level was 1.19 m and the prediction is 1.15 m; in October 29, 2012, when Hurricane Sandy ("S" in Fig. 11) was offshore, the observed water level was 1.22 m and the prediction was 1.35 m; in October 4, 2015, when Hurricane Joaquin ("J" in Fig. 11) was offshore, the observed water level was 1.14 m and the prediction is 1.6 m (the latest

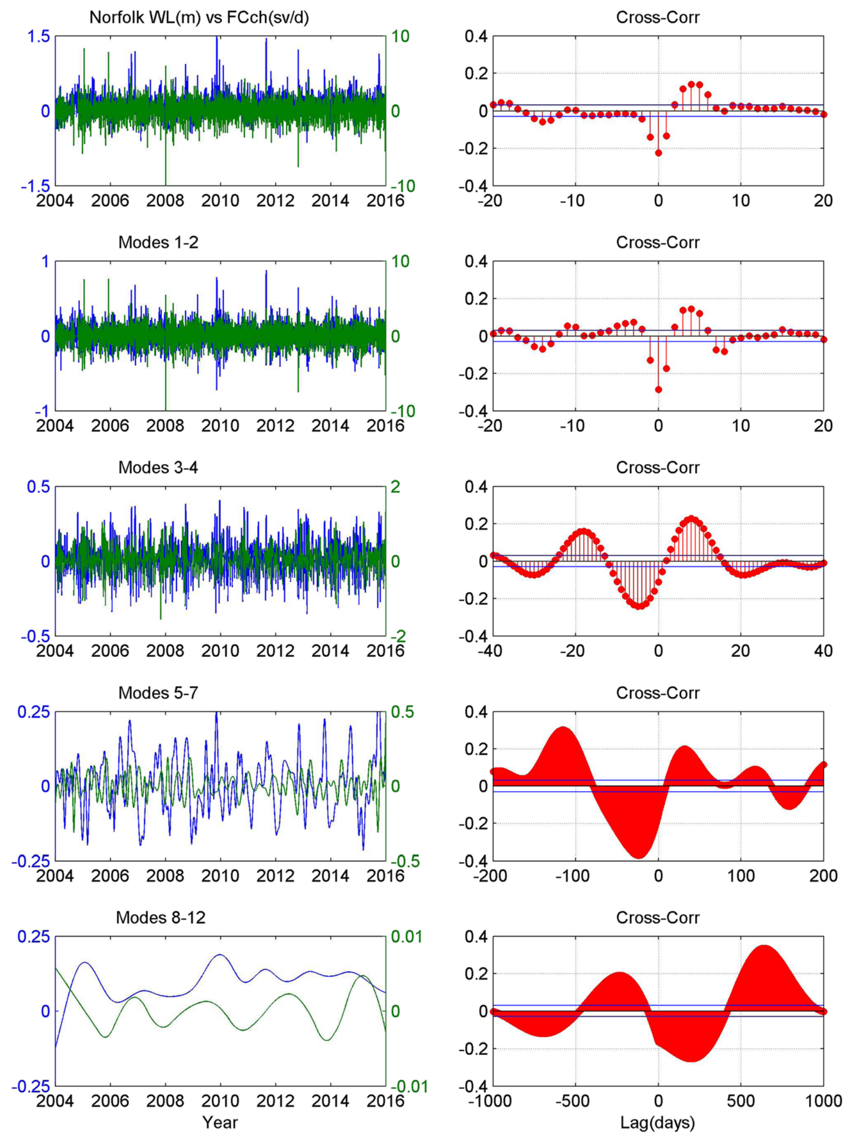

Fig. 7 Same as Fig. 4, but comparing water level in Norfolk versus FCT change (Sv/day) instead of FC itself

hurricane will be discussed in more details in the next section). However, the prediction is not so accurate for a fast-moving hurricane like Irene ("I" in Fig. 11) that passed almost directly over Norfolk in August 28, 2011, so it did not affect the offshore Gulf Stream that much. In the case of Hurricane Irene, the observed water level was 1.46 m and the predicted water level is only 0.6 m, indicating that the storm surge was mostly due to direct wind forcing, while in the other cases, offshore storms affected the Gulf Stream and added an indirect impact to coastal sea level.

4 An example of remote influence: Hurricane Joaquin (2015)

As seen in Fig. 2a, years with considerable flooding are clustered over the past decade or so—the reason is that storms that in the past caused little or no damage are now causing longer and more severe flooding due to the addition of sea level rise (Ezer and Atkinson 2014; Sweet and Park 2014). The third most flooded year on record in Norfolk was 2015, and the majority of the flooding this year occurred during about 2 weeks in late September to early October when Hurricane Joaquin was developing in the tropics (Fig. 2b). Despite the fact that this hurricane moved northeastward away from the coast and never made a landfall (Fig. 2c), it caused severe flooding along the US coasts (additional precipitation from a weather front also added to flooding). This storm seemed to impact the transport of the FCT, so it is presented here as an example of remote influence on coastal sea level. Figure 12a shows the hourly water level at Norfolk for June–October, 2015. The observed water level (red line) was above the tide prediction (blue) for much of this period (green represents the residual, i.e., observed minus predicted), with particular high

Fig. 8 Correlation coefficient between water level and FCT (*left panels*) and lag for the maximum correlation (*right panels*), for the high-frequency modes (*top*) and low-frequency modes (*bottom panels*). Negative lag means that FCT variations are ahead of water-level variations. The 12 stations are listed from north to south except the offshore station in Bermuda (see Fig. 1)

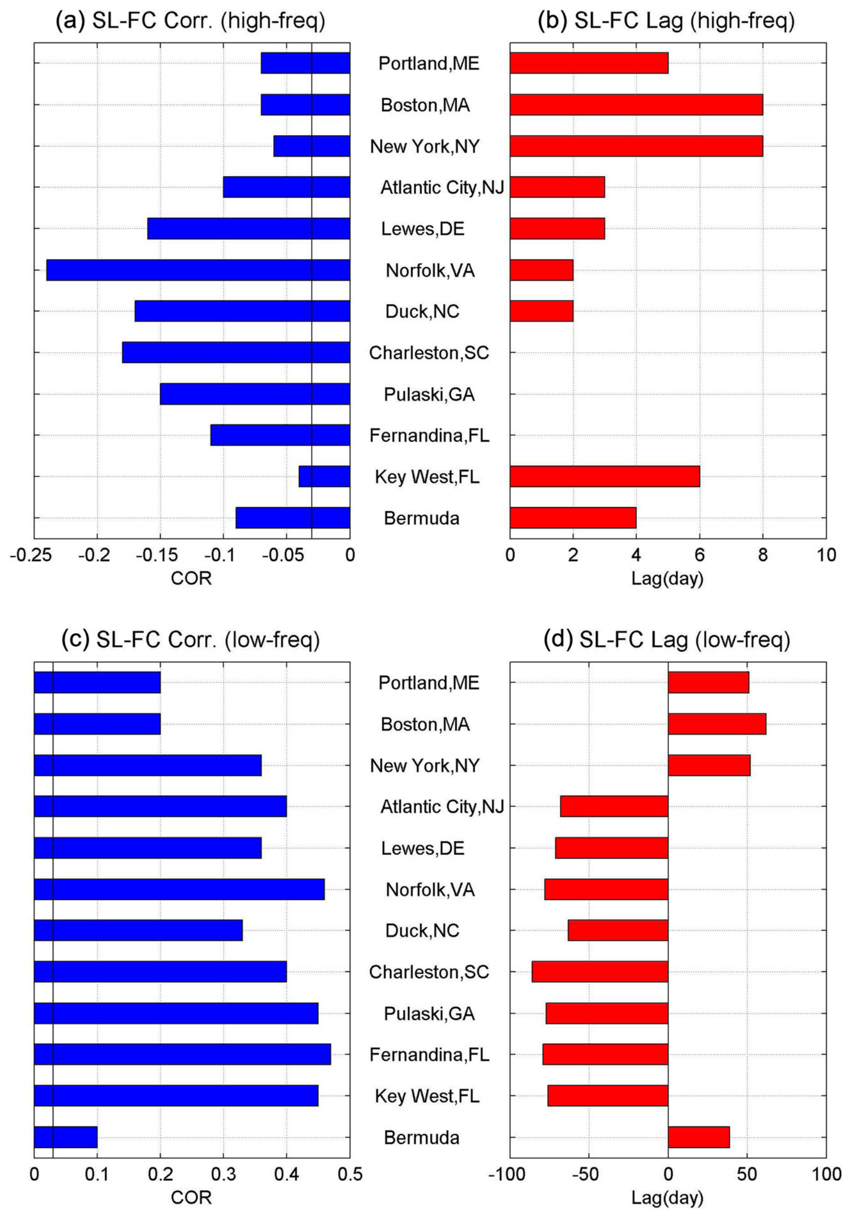

waters (~1 m above MHHW) in late September to early October; luckily enough, the highest water level occurred during neap tide; nevertheless, Norfolk streets were flooded almost every high tide during this 2-week period. Figure 12b, c compares the daily water level anomaly with the daily FCT (in Sv) and FCC (in Sv per day), respectively. The correlations with FCT (−0.39) and FCC (−0.28) are statistically significant at 99% confidence level and indicate that ~15 and ~8% of the variability is represented by the FCT and FCC, respectively. As mentioned before (Fig. 10), higher correlations will be obtained if only the highest water levels are considered. The most interesting result is the fact that the hurricane caused about 30% reduction in the FCT—this is consistent with the location of the hurricane (Fig. 2b) which would create southwestward flowing wind over the SAB, in opposite direction to the Florida Current. The two low-flow peaks in the FCT are accompanied by two peaks in anomalously high water, which is consistent with the previous findings that slower current would raise coastal water level. Note also that the FCC minima peaks predict not only the hurricane period but also other maxima peaks in water level (e.g., days 155, 220, 265, and 280, in Fig. 10c).

One may wonder, however, if storm surge due to local winds or low air pressure (and the inverter barometer effect) could have caused this high water level in late September (there was also a weather front moving over the area). Therefore, the local air pressure and wind speed from a meteorological station near Norfolk are shown in Fig. 12d. Pressure and wind are anti-correlated most of the time, but less so during the hurricane period. During late September,

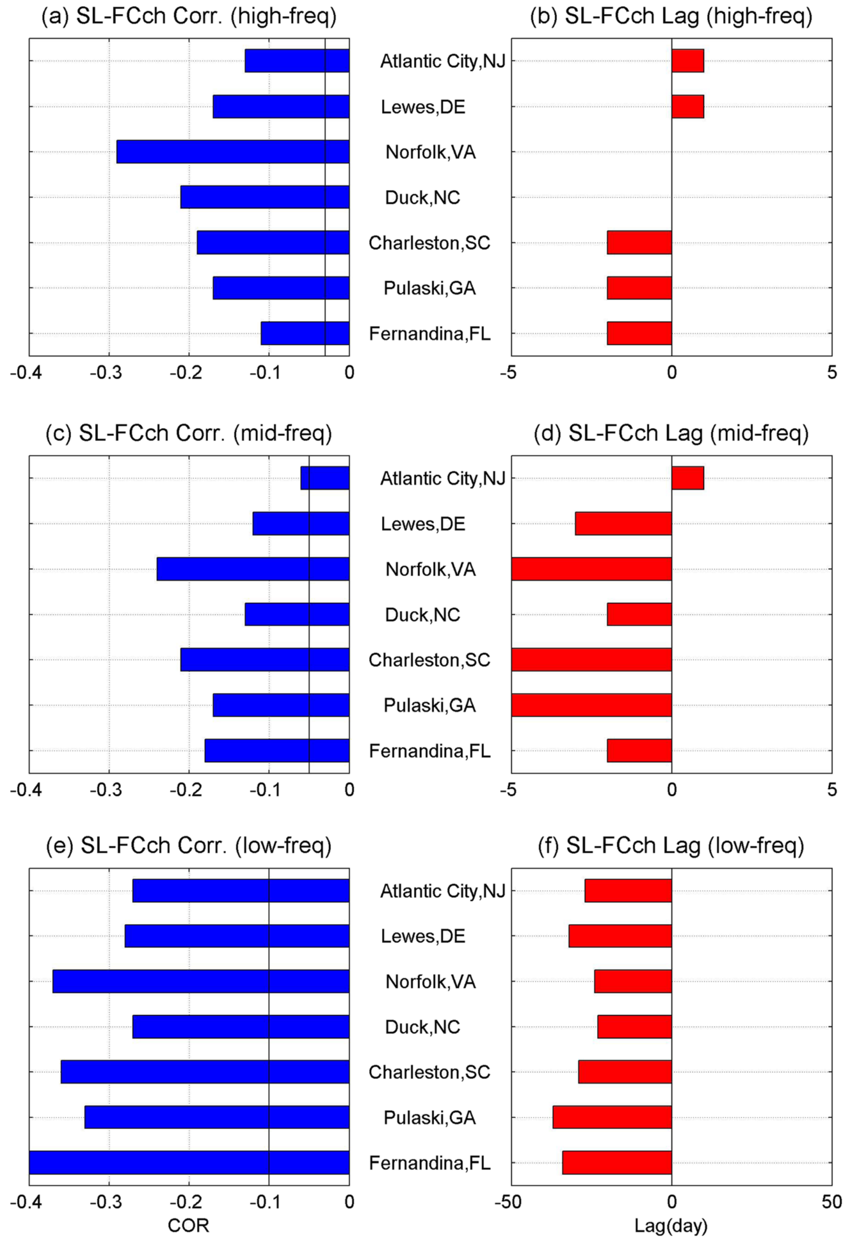

Fig. 9 Similar to Fig. 7, but only for the seven stations in the Mid-Atlantic and South Atlantic Bights. The correlations are between water level and FCT change for the three frequency bands

there are some variations in air pressure and wind stronger than before (probably due to the front mentioned above), but wind speed of 4–5 m s^{-1} cannot cause a storm surge of 1 m, so local wind can contribute somewhat to variations in water level but cannot explain the long period of high water and flooding. The local air pressure is not low enough to indicate any strong local storm over the region.

5 Summary and conclusions

Sea level rise and acceleration, especially in the mid-Atlantic region (Boon 2012; Sallenger et al. 2012; Ezer and Corlett 2012; Ezer 2013), is causing an acceleration in flooding in low-lying cities and coastal communities along the US East Coast (Mitchell et al. 2013; Ezer and Atkinson 2014; Sweet and Park 2014). It is also observed that minor tidal flooding can often occur without any wind or local weather event (so-called clear-day flooding), so that coastal water levels simulated by storm surge models are sometimes underpredicted be as much as 0.2–0.5 m. These problems may be attributed to non-local factors such as offshore variations in the Gulf Stream, westward-propagating planetary waves, and climatic variations in the North Atlantic Ocean. Since these remote influences cannot be captured by regional operational storm surge models that rely on local winds, CSL prediction may be improved in the future by including additional remote forcing; this will require the availability of observations such as

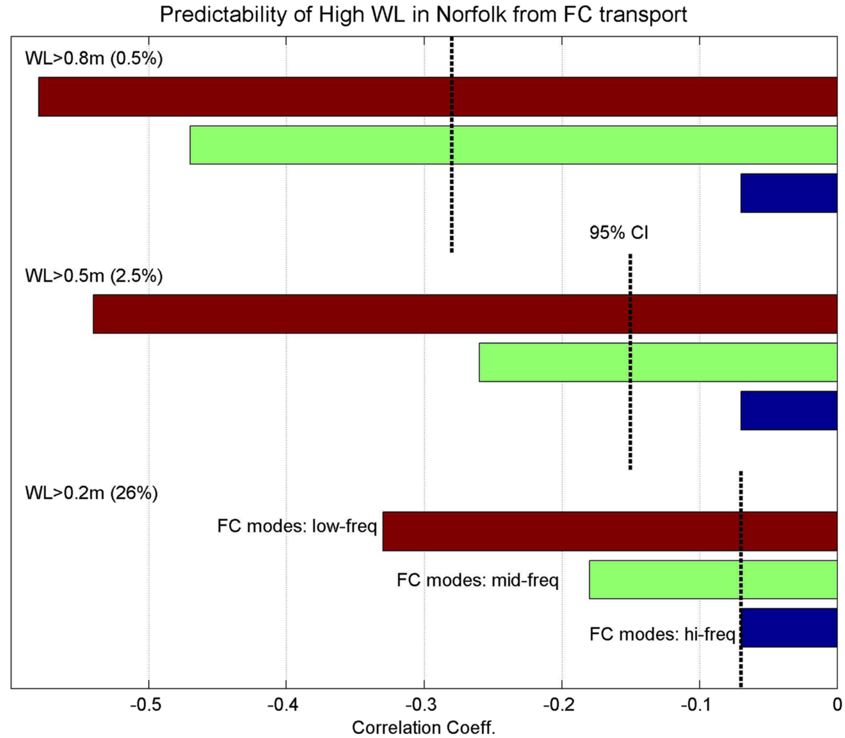

Fig. 10 Predictability of different levels of high water in Norfolk, using EMD modes of FCT for different frequencies: high, medium, and low frequency in *blue*, *green*, and *red* colors, respectively. Correlation is calculated for only those days with water level of 0.8, 0.5, and 0.2 m above MHHW (the % of the time these levels are reached during the 12-year period is indicated). The *vertical dashed lines* are estimated 95% confidence intervals. These correlations are for zero lag (if optimal lag for each case is considered, the correlations would be higher)

AMOC and FCT in real time and modifications of the models. The influence of the Gulf Stream on coastal sea level variability has been recognized in early observations (Montgomery 1938; Blaha 1984), but this remote impact is difficult to fully understand and quantify, so it attracts considerable interest and hypotheses (Levermann et al. 2005; Ezer 2001, 2013, 2016; Ezer et al. 2013; Sallenger et al. 2012; Goddard et al. 2015; Park and Sweet 2015). Since the Florida Current transport measurements are continuous, available daily, and represent some remote Atlantic Ocean variability, they are evaluated here for their usefulness to predict potential high water level along the coast. In particular, the study is set to evaluate the correlation between the FCT and high water level and to describe the spatial and temporal distribution of the correlations.

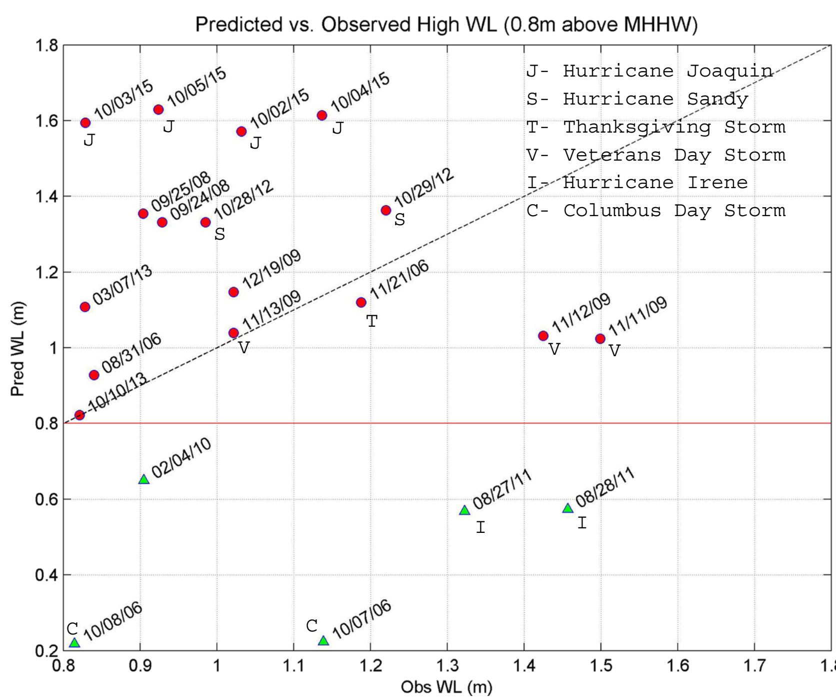

Fig. 11 Predicted and observed high water level for all the cases when daily water level in Norfolk reached 0.8 m above MHHW (during 2004–2015). The prediction is based on linear regression using the sea level-FC correlation of the low-frequency band in Fig. 10 (see text for details). The dates (month/day/year) and notable storms are indicated. The storm days when the prediction correctly shows high water level above 0.8 m are indicated by *red circles*, while underpredicted storms are indicated by *green triangles*

Fig. 12 **a** Hourly observed water level (*red*) tide prediction (*blue*) and residual anomaly (*green*) in Norfolk for June–October, 2015. **b** Daily FCT (*blue*) and water level anomaly (*green*). **c** Daily FCT change (*blue*) and water level anomaly (*green*). The anomalously high water level in mid-September to early October was during the time that hurricane Joaquin was developed (see Fig. 2b). **d** Daily air pressure (*green*) and wind speed (*blue*) from a meteorological station near Norfolk

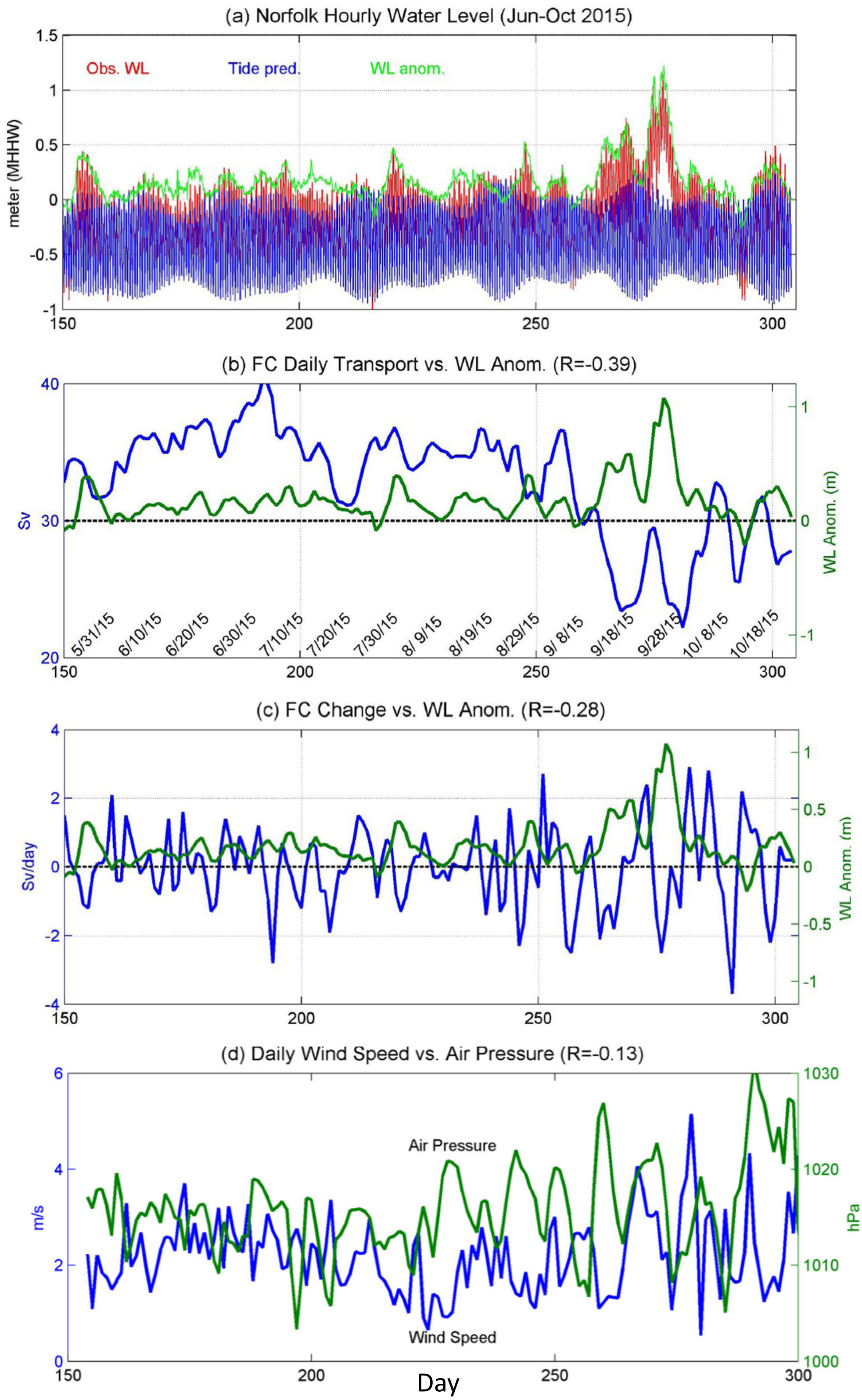

An EMD analysis is used to look at different timescales from few days to seasonal variations. Some statistically significant correlations have been found between the FCT and high water level along the entire US East Coast. It is estimated that ~10–25% of the variability in CSL may be attributed to the FCT variability. There is also a clear spatial pattern in correlation values and in time lags that indicates that the signals captured by the FCT are affected by topography and coastline and are propagating along the coast, as previously observed and modeled (Ezer 2016, 2017). The two predictive measures that are tested are FCT and FCT change (FCC), and in general, high water level is found when FCT is either weak or if it had a slowdown trend, which is consistent with basic physical oceanography principals and previous analysis (Ezer et al. 2013). Particular practical findings are the potential predictability of flooding in the lower MAB from the FCT observed at the same time and the fact that low-frequency EMD modes of FCT are most useful for predicting extreme events (water level as high as 0.8 m above MHHW is evaluated here). An example of remote forcing affecting the coasts is the case of Hurricane Joaquin (September–October, 2015), which demonstrates how an offshore storm can cause a weakening of the FCT and consequently an increase in the high water level that affect flooding along the US East Coast. This single storm was responsible for the majority of the flooding in 2015, making it the third most flooded year on record for cities such as Norfolk, VA. In general, it was found that hurricanes and storms that are either slow moving or remain offshore for some time have larger impact on the Gulf Stream, and thus, the remote forcing signal can be better predicted from the FCT data than other storms. The hope is that this study can help to improve water level prediction by using measurements such as FCT to account for remote forcing processes that are not directly observed and difficult to include in storm surge models.

Acknowledgements Old Dominion University's Climate Change and Sea Level Rise Initiative (CCSLRI) provided partial support for this study, and the Center for Coastal Physical Oceanography (CCPO) provided computational support. The hourly tide gauge sea level data are available from http://opendap.co-ops.nos.noaa.gov/dods/. The Florida Current transport data is obtained from http://www.aoml.noaa.gov/phod/floridacurrent/.

References

Baringer MO, Larsen JC (2001) Sixteen years of Florida current transport at 27N. Geophys Res Lett 28(16):3,179–3,182

Berg R (2016) Hurricane Joaquin 28 September–7 October, 2015. National Hurricane Center Tropical Cyclone Report. NOAA/NHC, 36 pp

Blaha JP (1984) Fluctuations of monthly sea level as related to the intensity of the Gulf Stream from Key West to Norfolk. J Geophys Res Oceans 89(C5):8033–8042

Boon JD (2012) Evidence of sea level acceleration at U.S. and Canadian tide stations, Atlantic coast, North America. J Coast Res 28(6): 1437–1445. doi:10.2112/JCOASTRES-D-12-00102.1

Chen X, Feng Y, Huang NE (2014) Global sea level trend during 1993–2012. Glob Plan Change 112:26–32. doi:10.1016/j.gloplacha.2013.11.001

Domingues R, Baringer M, Goni G (2016) Remote sources for year-to-year changes in the seasonality of the Florida Current transport. J Geophys Res 121(10):7547–7559. doi:10.1002/2016JC012070

Eggleston J, Pope J (2013) Land subsidence and relative sea-level rise in the southern Chesapeake Bay region. Report No. 1392, US Geological Survey, 30pp. doi:10.3133/cir1392

Ezer T (1999) Decadal variabilities of the upper layers of the subtropical North Atlantic: an ocean model study. J Phys Oceanogr 29(12): 3111–3124. doi:10.1175/1520-0485(1999)029

Ezer T (2001) Can long-term variability in the Gulf Stream transport be inferred from sea level? Geophys Res Lett 28(6):1031–1034. doi:10.1029/2000GL011640

Ezer T (2013) Sea level rise, spatially uneven and temporally unsteady: why the U.S. East Coast, the global tide gauge record, and the global altimeter data show different trends. Geophys Res Lett 40:5439–5444. doi:10.1002/2013GL057952

Ezer T (2015) Detecting changes in the transport of the Gulf Stream and the Atlantic overturning circulation from coastal sea level data: the extreme decline in 2009-2010 and estimated variations for 1935-2012. Glob Planet Change 129:23–36. doi:10.1016/j.gloplacha.2015.03.002

Ezer T (2016) Can the Gulf Stream induce coherent short-term fluctuations in sea level along the U.S. East Coast?: A modeling study, Ocean Dyn 66(2):207–220. doi:10.1007/s10236-016-0928-0

Ezer T (2017) A modeling study of the role that bottom topography plays in Gulf Stream dynamics and in influencing the tilt of mean sea level along the U.S. East Coast. Ocean Dyn. doi:10.1007/s10236-017-1052-5

Ezer T, Atkinson LP (2014) Accelerated flooding along the U.S. East Coast: on the impact of sea-level rise, tides, storms, the Gulf Stream, and the North Atlantic Oscillations. Earth's Future 2(8): 362–382. doi:10.1002/2014EF000252

Ezer T, Corlett WB (2012) Is sea level rise accelerating in the Chesapeake Bay? A demonstration of a novel new approach for analyzing sea level data. Geophys Res Lett 39:L19605. doi:10.1029/2012GL053435

Ezer T, Atkinson LP, Corlett WB, Blanco JL (2013) Gulf Stream's induced sea level rise and variability along the U.S. mid-Atlantic coast. J Geophys Res 118:685–697. doi:10.1002/jgrc.20091

Ezer T, Haigh ID, Woodworth PL (2015) Nonlinear sea-level trends and long-term variability on western European coasts. J Coastal Res. doi:10.2112/JCOASTRES-D-15-00165.1

Goddard PB, Yin J, Griffies SM, Zhang S (2015) An extreme event of sea-level rise along the northeast coast of North America in 2009–2010. Nature Comm 6:6346. doi:10.1038/ncomms7346

Huang NE, Shen Z, Long SR, Wu MC, Shih HH, Zheng Q, Yen N-C, Tung CC, Liu HH (1998) The empirical mode decomposition and the hilbert spectrum for non stationary time series analysis. Proc Roy Soc Lond 454:903–995

Hughes CW, Meredith PM (2006) Coherent sea-level fluctuations along the global continental slope. Philos Trans R Soc 364:885–901. doi:10.1098/rsta.2006.1744

Huthnance JM (2004) Ocean-to-shelf signal transmission: a parameter study. J Geophys Res 109:C12029. doi:10.1029/2004JC002358

Karegar MA, Dixon TH, Engelhart SE (2016) Subsidence along the Atlantic Coast of North America: insights from GPS and late Holocene relative sea level data. Geoph Res Lett 43:3126–3133. doi:10.1002/2016GL068015

Levermann A, Griesel A, Hofmann M, Montoya M, Rahmstorf S (2005) Dynamic sea level changes following changes in the thermohaline circulation. Clim Dyn 24(4):347–354

McCarthy G, Frejka-Williams E, Johns WE, Baringer MO, Meinen CS, Bryden HL, Rayner D, Duchez A, Roberts C, Cunningham SA (2012) Observed interannual variability of the Atlantic meridional overturning circulation at 26.5oN. Geophys Res Lett 39(19). doi:10.1029/2012GL052933

Meinen CS, Baringer MO, Garcia RF (2010) Florida current transport variability: an analysis of annual and longer-period signals. Deep Sea Res 57(7):835–846. doi:10.1016/j.dsr.2010.04.001

Miller KG, Kopp RE, Horton BP, Browning JV, Kemp AC (2013) A geological perspective on sea-level rise and its impacts along the US mid-Atlantic coast. Earth's Future 1(1):3–18. doi:10.1002/2013EF000135

Mitchell, M, Hershner C, Herman J, Schatt D, Eggington E, Stiles S (2013) Recurrent flooding study for Tidewater Virginia, Rep. SJR 76, 2012, 141 pp., Va. Inst. of Marine Sci., Gloucester Point, Va

Montgomery R (1938) Fluctuations in monthly sea level on eastern U.S. coast as related to dynamics of western North Atlantic Ocean. J Mar Res 1:165–185

Park J, Sweet W (2015) Accelerated sea level rise and Florida Current transport. Ocean Sci 11:607–615. doi:10.5194/os-11-607-2015

Piecuch CG, Ponte RM (2015) Inverted barometer contributions to recent sea level changes along the northeast coast of North America. Geophys Res Lett 42(14):5918–5925. doi:10.1002/2015GL064580

Piecuch C, Dangendorf S, Ponte R, Marcos M (2016) Annual sea level changes on the North American Northeast Coast: influence of local winds and barotropic motions. J Clim 29:4801–4816. doi:10.1175/JCLI-D-16-0048.1

Rossby T, Flagg C, Donohue K (2010) On the variability of Gulf Stream transport from seasonal to decadal timescales. J Mar Res 68:503–522. doi:10.1357/002224010794657128

Sallenger AH, Doran KS, Howd P (2012) Hotspot of accelerated sea-level rise on the Atlantic coast of North America. Nature Clim Change 2:884–888. doi:10.1038/NCILMATE1597

Smeed DA, McCarthy G, Cunningham SA, Frajka-Williams E, Rayner D, Johns WE, Meinen CS, Baringer MO, Moat BI, Duchez A, Bryden HL (2013) Observed decline of the Atlantic Meridional Overturning Circulation 2004 to 2012. Ocean Sci Discus 10:1619–1645. doi:10.5194/osd-10-1619-2013

Srokosz MA, Bryden HL (2015) Observing the Atlantic Meridional Overturning Circulation yields a decade of inevitable surprises. Science 348(6241). doi:10.1126/science.1255575

Sturges WB, Hong G (2001) Gulf Stream transport variability at periods of decades. J Phys Oceanogr 31:1304–1312

Sweet W, Park J (2014) From the extreme to the mean: acceleration and tipping points of coastal inundation from sea level rise. Earth's Future 2(12):579–600

Thiebaux HJ, Zwiers FW (1984) The interpretation and estimation of effective sample size. J Clim Appl Meteor 23:800–811

Thomson RE, Emery WJ (2014) Time series analysis methods, in data analysis methods in physical oceanography, Third edn. Elsevier, Boston, pp 425–591. doi:10.1016/B978-0-12-387782-6.00005-3

Woodworth PL., Maqueda MM, Gehrels WR, Roussenov VM, Williams RG, Hughes CW (2016) Variations in the difference between mean sea level measured either side of Cape Hatteras and their relation to the North Atlantic Oscillation. Clim Dyn 1–19. doi: 10.1007/s00382-016-3464-1

Yin J, Goddard PB (2013) Oceanic control of sea level rise patterns along the East Coast of the United States. Geophys Res Lett 40:5514–5520. doi:10.1002/2013GL057992

Zhao J, Johns W (2014) Wind-forced interannual variability of the Atlantic Meridional Overturning Circulation at 26.5°N. J Geophys Res Oceans 119:6253–6273. doi:10.1002/2013JC009407